Accepted Manuscript

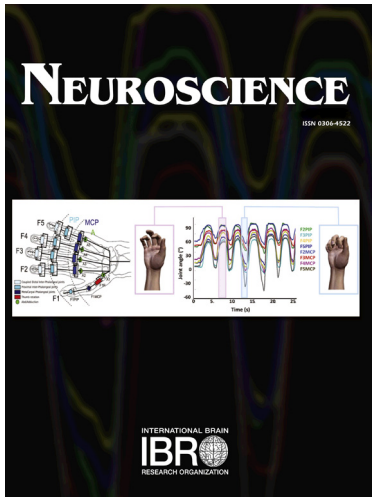


Intrathecal application of the microglial inhibitor minocycline attenuates sympathoexcitatory and proarrhythmogenic changes in rats with chronic temporal lobe epilepsy

Amol M. Bhandare, Komal Kapoor, Kim L. Powell, Emma Braine, Pablo Casillas-Espinosa, Terence J. O'Brien, Melissa M.J. Farnham, Paul M. Pilowsky

PII: S0306-4522(17)30170-7
DOI: http://dx.doi.org/10.1016/j.neuroscience.2017.03.012
Reference: NSC 17656

To appear in: *Neuroscience*

Received Date: 20 December 2016
Revised Date: 2 March 2017
Accepted Date: 7 March 2017

Please cite this article as: A.M. Bhandare, K. Kapoor, K.L. Powell, E. Braine, P. Casillas-Espinosa, T.J. O'Brien, M.M.J. Farnham, P.M. Pilowsky, Intrathecal application of the microglial inhibitor minocycline attenuates sympathoexcitatory and proarrhythmogenic changes in rats with chronic temporal lobe epilepsy, *Neuroscience* (2017), doi: http://dx.doi.org/10.1016/j.neuroscience.2017.03.012

# Intrathecal application of the microglial inhibitor minocycline attenuates sympathoexcitatory and proarrhythmogenic changes in rats with chronic temporal lobe epilepsy

Amol M. Bhandare,[1,2,5] Komal Kapoor,[1,2] Kim L. Powell,[4] Emma Braine,[4] Pablo Casillas-Espinosa,[4] Terence J. O'Brien,[4] Melissa M. J. Farnham,[2,3] and Paul M. Pilowsky[2,3]*

[1]Faculty of Medicine and Health Sciences, Macquarie University, Sydney, 2109 New South Wales, Australia, [2]The Heart Research Institute, 7 Eliza Street, Sydney, 2042 New South Wales, Australia, [3]Department of Physiology, University of Sydney, Sydney, 2006 New South Wales, Australia, [4]Department of Medicine, The Royal Melbourne Hospital, The University of Melbourne, Parkville, Victoria, Australia and [5]School of Life Sciences, University of Warwick, Coventry CV4 7AL, United Kingdom.

Corresponding author: Paul M. Pilowsky (paul.pilowsky@hri.org.au)

Address: The Heart Research Institute, 7 Eliza Street, Sydney, 2042 New South Wales, Australia

Tel: +61 2 8208 8900 Fax: +61 2 9517 1552

Co-authors' email addresses:

| | |
|---|---|
| Amol M. Bhandare: | bhandaream@gmail.com |
| Komal Kapoor: | contactkomalk@gmail.com |
| Kim L. Powell: | kpowell@unimelb.edu.au |
| Emma Braine: | ebraine@unimelb.edu.au |
| Pablo Casillas-Espinosa: | pablo.casillas@unimelb.edu.au |
| Terence J. O'Brien: | obrientj@unimelb.edu.au |
| Melissa M. J. Farnham: | melissa.farnham@hri.org.au |

Conflict of interest: Authors have no conflicts of interest to declare.

**List of Abbreviations:**

| | |
|---|---|
| SUDEP: | sudden unexpected death in epilepsy |
| PACAP: | pituitary adenylate cyclase-activating polypeptide |
| IML: | intermediolateral cell column |
| RVLM: | rostral ventrolateral medulla |
| SNA: | sympathetic nerve activity |
| SE: | status epilepticus |
| QT interval: | a measure of the time between the start of the Q wave and the end of the T wave in the heart's electrical cycle |
| KA: | kainic acid |
| TLE: | temporal lobe epilepsy |
| Post-SE: | post-status epilepticus |
| IT: | intrathecal |
| ECG: | electrocardiogram |
| O.D.: | outer diameter |
| HR: | heart rate |
| PBS: | phosphate-buffered saline |
| TH: | tyrosine hydroxylase |
| CD: | cluster of differentiation |
| Iba1: | iodinised calcium binding adaptor molecule-1 |
| AUC: | area under curve |
| MAP: | mean arterial pressure |
| PaCO2: | partial pressure of carbon dioxide |
| QTc: | corrected QT interval |
| ir: | immunoreactive |

**Abstract:**

The incidence of sudden unexpected death in epilepsy (SUDEP) is highest in people with chronic and drug resistant epilepsy. Chronic spontaneous recurrent seizures cause cardiorespiratory autonomic dysfunctions. Pituitary adenylate cyclase-activating polypeptide (PACAP) is neuroprotective, whereas microglia produce both pro- and anti- inflammatory effects in the CNS. During acute seizures in rats, PACAP and microglia produce sympathoprotective effect at the intermediolateral cell column (IML), whereas their action on the presympathetic rostral ventrolateral medulla (RVLM) neurons mediates proarrhythmogenic changes. We evaluated the effect of PACAP and microglia at the IML on sympathetic nerve activity (SNA), cardiovascular reflex responses, and electrocardiographic changes in the post-status epilepticus (SE) model of acquired epilepsy, and control rats. Chronic spontaneous seizures in rats produced tachycardia with profound proarrhythmogenic effects (prolongation of QT interval). Antagonism of microglia, but not PACAP, significantly reduced the SNA and the corrected QT interval in post-SE rats. PACAP and microglia antagonists did not change baroreflex and peripheral or central chemoreflex responses with varied effect on somatosympathetic responses in post-SE and control rats. We did not notice changes in microglial morphology or changes in a number of M2 phenotype in epileptic nor control rats in the vicinity of RVLM neurons. Our findings establish that microglial activation, and not PACAP, at the IML accounts for higher SNA and proarrhythmogenic changes during chronic epilepsy in rats. This is the first experimental evidence to support a neurotoxic effect of microglia during chronic epilepsy, in contrast to their neuroprotective action during acute seizures.

**Keywords:**

Microglia, Sympathoexcitation, Temporal lobe epilepsy, Rats, Proarrhythmogenic, PACAP

**Introduction:**

Epilepsy is a chronic brain disorder characterised by spontaneous recurrent seizures and carries a risk of sudden death that is 15-20 times higher than in normal population (Ficker et al., 1998; Nilsson et al., 1999; Eastaugh et al., 2015). Epilepsy affects about 50 million people worldwide (WHO, 2005); seizures can range from brief, barely noticeable loss of attention to major convulsions that affect the entire neuraxis. Epilepsy is associated with changes in autonomic functions, such as sympathovagal imbalance, sympathetic reflex dysfunction, tachycardia with concomitant arrhythmia or bradycardia with associated apnoea (Dütsch et al., 2006; Bateman et al., 2008; Ponnusamy et al., 2012; Massey et al., 2014; Powell et al., 2014b; Bhandare et al., 2015; Bhandare et al., 2016a). Seizure associated autonomic cardiorespiratory changes are well-documented and are thought to play an important role in a mechanism of sudden unexpected death in epilepsy (SUDEP) (Nei et al., 2004; Dlouhy et al., 2015). Interictal autonomic changes are also seen in patients with chronic epilepsy (Ansakorpi et al., 2000; Berilgen et al., 2004; Müngen et al., 2010; Lotufo et al., 2012). Nevertheless, the neuronal mechanisms causing autonomic cardiorespiratory dysfunction during chronic epilepsy are unknown.

Pituitary adenylate cyclase-activating polypeptide (PACAP), a 38 amino acid pleiotropic neuropeptide, produce neuroprotective effects (Shioda et al., 1998; Ohtaki et al., 2006; Bhandare et al., 2015) that are partly mediated through its action on microglia (Wada et al., 2013; Brifault et al., 2015). PACAP and microglia have a protective effect on sympathetic preganglionic neurons at the intermediolateral cell column (IML), where they ameliorate the sympathoexcitatory effect of acute seizures (Bhandare et al., 2015). During acute seizures, PACAP and microglia act on presympathetic rostral ventrolateral medulla (RVLM) neurons in the brainstem to promote proarrhythmogenic changes, but not sympathoexcitation (Bhandare et al., 2016a). In many cardiovascular autonomic nuclei PACAP is pressor and sympathoexcitatory (Farnham et al., 2008; Farnham et al., 2011; Inglott et al., 2011) and changes baroreflex response in trout (Lancien et al., 2011) but not in rats (Farnham et al., 2012). PACAP expression is increased in central autonomic nuclei (paraventricular nucleus) after kainic acid (KA)-induced seizures in rats (Nomura et al., 2000). Secondly, seizures produce microglial activation, and neuroinflammation

in patients and animal models (Beach et al., 1995; Shapiro et al., 2008; Eyo et al., 2014), which persist for many years during chronic epilepsy (Beach et al., 1995; Papageorgiou et al., 2015). Microglia can be pro- or anti- inflammatory in animal models of temporal lobe epilepsy (TLE) (Shapiro et al., 2008; Mirrione et al., 2010; Vinet et al., 2012; Devinsky et al., 2013). Although the pro- or anti- inflammatory state of activated microglia is a topic of debate, there is strong support for their dual role (Hanisch and Kettenmann, 2007). Short term microglial activation is considered beneficial (Mirrione et al., 2010; Vinet et al., 2012; Szalay et al., 2016), whereas chronic microglial activation is deleterious, and produces a damaging response to injury (Qin et al., 2007; Loane et al., 2014; Olmos-Alonso et al., 2016). During KA-induced acute seizures, spinal microglia have a protective effect on sympathetic preganglionic neurons (Bhandare et al., 2015), however, their role in chronic epilepsy is not known.

Thus, the aims of this study were to identify the role of PACAP and microglia in the spinal cord, during chronic epilepsy, in the regulation of central autonomic cardiovascular activity. To achieve these aims we used a model of acquired epilepsy in rats that manifest spontaneous seizures and many features of acquired epilepsy in humans– the KA-induced post-status epilepticus (post-SE) model (Morimoto et al., 2004; Powell et al., 2008; Jupp et al., 2012). The effect of intrathecal (IT) infusion of the PACAP antagonist, PACAP(6-38), and the microglial antagonist, minocycline, on sympathetic activity, cardiovascular reflex responses, and the electrocardiogram (ECG) were analysed in chronically epileptic and control rats. Microglial morphology and their phenotype in the vicinity of RVLM neurons were analysed with immunohistochemistry in epileptic and control rats.

**Experimental Procedures:**

**Animals**

The animal usage and protocols were in accordance with the Australian code of practice for the care and use of animals for scientific purposes. The protocols were approved by the Animal Care, and Ethics Committee of Macquarie University, The University of Melbourne, and the Sydney Local Health District. The epilepsy surgery and procedures were performed under isoflurane anesthesia on 17-19 weeks old

adult non-epileptic control (*n* = 9), and post-SE (*n* = 15) male Wistar rats, whereas electrophysiology experiments were performed under urethane anesthesia.

**KA-induced post-SE rat model**

The post-SE model of acquired epilepsy was generated by i.p. injection of the glutamate receptor agonist, KA, to induce a period of continuous seizure activity (status epilepticus) in non-epileptic rats as described previously (Hellier et al., 1998; Powell et al., 2008; Jupp et al., 2012; Powell et al., 2014b; Vivash et al., 2014). Twelve week old Wistar rats were injected with repeated low doses of KA (5mg/kg, i.p., followed by 2.5 mg/kg, i.p., injections once per hour) until SE behaviour was observed. After four hours of SE, all rats were given diazepam injection (5mg/kg i.p.) to terminate the SE. Rats were then returned to their home cages in the animal house and maintained with normal animal house care and diet.

**Implantation of EEG-ECG electrodes in post-SE and control rats**

Seven weeks after KA-induced SE (*n* = 15) (or saline administered controls (*n* = 9)), two ECG electrodes and four EEG electrodes were implanted in each rat under isoflurane anesthesia (5% during induction, 2.5-1.5% for maintenance) in oxygen (2.0 L/min during induction, 0.5-1.0 L/min for maintenance) as detailed in supporting data by (Powell et al., 2014b). Two small incisions were made to expose the thoracic muscle directly above the heart, and to expose the muscle overlying the xiphoid process of the sternum. The distal end of an ECG lead (13 cm; PlasticsOne, USA) was sutured to each muscle using polypropylene, 4-0 (Sharpoint, USA). The leads of both ECG electrodes were then tunnelled up through the left side of the neck subcutaneously, and the skin layer was sutured (polyglycolic, 4-0; LOOK™, USA). A single midline incision was then made on the scalp to expose the skull. Two ECG leads were located and tunneled through the neck to allow protrusion of the leads out of the incision site on the scalp. Each rat was then placed into a stereotaxic frame, and four extradural electrodes comprised of gold-plated sockets attached to stainless steel screws (O.D. 1 mm; Plastics One, USA) were implanted into the skull: one on each side approximately 2 mm from the midline, 3 mm anterior to the Bregma, one at approximately the centre of the midline, and another 6 mm posterior to the Bregma, 4 mm right of the midline. The electrodes were fixed to the skull using dental cement (Vertex-Dental, The Netherlands), and the animals observed until recovery.

***In vivo* EEG-ECG recordings**

One week after recovery from the surgery, a continuous 24 h video-EEG-ECG recording was acquired for one week using Compumedics EEG acquisition software (Profusion EEG 4 v4.3, Australia) digitised at 2048Hz as previously described (Powell et al., 2008; Powell et al., 2014b). Each recording was reviewed for seizure activity, and the start and end of a seizure was manually marked on the EEG to allow quantification of the number of seizures and seizure duration. Seizure activity on the EEG was defined as per our previous work, and that of others, as the development of high-amplitude, rhythmic discharges that clearly represented a new pattern of tracing (Kharatishvili et al., 2006; Bouilleret et al., 2011). This included repetitive spikes, spike-and-wave discharges, and slow waves. The event must have lasted at least 5 s and showed an evolution in the dominant frequency, and be accompanied by behavioural change observable on the video recording consistent with a seizure. Normally, all post-SE rats develop spontaneous seizures, and none were observed in control rats.

**Non-invasive tail-cuff blood pressure recordings**

A week after confirmation of spontaneous recurrent seizures in post-SE rats with video-EEG recordings and in age-matched controls, blood pressure was recorded with a non-invasive tail-cuff method (IITC Life Sciences Inc., California, USA) (Farnham et al., 2011). Rats were placed in an animal holder, pre-warmed at $32^0$C, and acclimatised to the chamber. All animals were kept in the chamber for 10-15 min; a cuff was attached to their tail, and blood pressure was recorded in triplicate and averaged. Heart rate (HR) and systolic, diastolic, and mean blood pressure was derived from the blood pressure waveform channel.

***In vivo* electrophysiology**

***General surgical procedure:*** Electrophysiology surgical procedures were carried out as described previously (Bhandare et al., 2015). Briefly, rats ($n$ = 24) were anesthetised with intraperitoneal injection of 10% urethane (ethyl carbamate; 1.3–1.5 g/kg; Sigma-Aldrich). The depth of anaesthesia was controlled by periodic tail/paw pinches and observing reflex responses (withdrawal or pressor >10 mmHg). When reflex responses were observed, an additional anaesthetic was injected (30-40 mg,

10% urethane intravenous). Bronchial secretion was prevented through administration of atropine sulphate (100 µg/kg, i.p.; Pfizer (Perth) Pty Limited, WA, Australia) with the first dose of anaesthetic.

The jugular vein and right carotid artery were cannulated for the administration of drugs and fluids, and for the recording of blood pressure, respectively. Tracheostomy enabled a mechanical ventilation. ECG was recorded through three lead electrodes, where two silver electrodes were inserted into the front paws and ground electrode into the exposed muscle on the back of rat. HR was derived from the peak of the R wave and drawn as an event channel. The head mounted EEG electrodes for *in vivo* EEG-ECG recordings enabled the recording of EEG signal. After bilateral cervical vagotomy rats were artificially ventilated (Ugo Basile, Italy) with 100% oxygen in order to silence the peripheral chemoreceptors. Rats were paralysed with pancuronium bromide (0.4 mg given as a 0.2 ml bolus i.v. injection) followed by an infusion of 10% pancuronium in 0.9% saline at a rate of 2 ml/h for the duration of the experiment. Rats were then secured in a stereotaxic frame and body temperature was maintained between 36.5 and 37.5$^0$C until the end of experiment with the use of a rectal probe and a homeothermic blanket (TC-1000; CWE). Arterial blood gases and electrolytes were analysed with an electrolyte and blood gas analyser (IDEXX Vetstat, West Brook, USA), and pH was maintained between 7.35 - 7.45 and $PaCO_2$ at 40 ± 2.

***IT catheter placement:*** The muscle layer attached to the occipital bone was carefully scraped with the cotton swabs to expose the membrane over the atlanto-occipital junction. The slit was made through the membrane and the surge of cerebrospinal fluid (CSF) provided the confirmation of correct site and was stopped by holding dry cotton swab. A polyethylene tubing (O.D. = 0.50 mm; I.D. = 0.20 mm; Microtube Extrusions Pty Ltd, NSW, Australia) with a dead space of ~6 µl was inserted through a slit in the dura into the IT space of all rats and advanced caudally to the level of T5/6.

***IT drug administration protocol:*** In all groups, drugs were administered intrathecally 10 min after recording of baseline reflex responses and flushed in with 6µl of phosphate-buffered saline (PBS). In both post-SE (*n* = 5) and control (*n* = 3) rats, 10 µl of a control injection of 10 mmol/l PBS, 1 mmol/l PACAP(6-38) or

100µg/10µl minocycline was administered intrathecally. All infusions were made over a 10 to 15 s period, as previously described (Bhandare et al., 2015).

***Isolation and preparation of nerves:*** The procedures were performed as described previously (Abbott and Pilowsky, 2009; Farnham et al., 2011; Inglott et al., 2011; Shahid et al., 2011). The left phrenic nerve and the left greater splanchnic sympathetic nerve at a site proximal to the coeliac ganglion were isolated and dissected. The dissected nerves were cut and the distal ends were tied with 5/0 silk thread. The isolated phrenic and splanchnic nerves were placed across a bipolar stainless steel electrodes and recorded. The nerves were electrically isolated either with paraffin oil or silgel. Signals were amplified (CWE, Incorporated, BMA-931 Bioamplifiers) (sampling rate: 6 kHz, gain: 2,000, filtering: 30-3,000Hz) and noise was removed with a 50/60-Hz line frequency filter (Humbug; Quest Scientific). The sciatic nerve was isolated at the mid-thigh, tied with 5/0 silk thread, and cut distally. The left aortic depressor nerve was isolated from the cervical vagus nerve at the level of the carotid bifurcation, tied with 5/0 silk thread and cut close to the chest.

***Aortic depressor and sciatic nerve stimulation and chemoreflexes protocol:*** The effect of aortic depressor and sciatic nerve stimulation on splanchnic sympathetic nerve activity (SNA) was assessed to estimate the baroreflex and somatosympathetic reflex function in post-SE and control rats in described previously (Miyawaki et al., 2001; Abbott and Pilowsky, 2009). Stimuli were generated by isolated stimulators controlled by a Spike2 script (version 8.03; Cambridge Electronic Design). Stimulus threshold was determined by increasing or decreasing the stimulus voltage until no response was observed. During each experimental protocol, the aortic depressor nerve was stimulated at 4 times threshold (1-10 V, 0.2-ms pulse width, 100 cycles at 1 Hz across 100 s), and the average SNA response was analysed before, and 60, 90 and 120 min after IT treatment (Fig. 1). The left sciatic nerve was stimulated to generate the somatosympathetic response. Stimulus threshold was determined as described above, and sciatic nerve was stimulated at 4 times threshold (1-5 V, 0.2 ms pulse width, 100 pulses at 0.4 Hz across 250 s), and the average response of SNA was analysed before, and 60, 90 and 120 min after IT treatment (Fig. 1).

Peripheral chemoreceptors were stimulated by ventilating animals with 10% $O_2$ in $N_2$ for 45 sec (Abbott and Pilowsky, 2009). Central chemoreceptors were stimulated by ventilating animals with 5% $CO_2$ / 95% $O_2$ for 3 min (Abbott and Pilowsky, 2009). The observed reflex responses are generated due to stimulation of central chemoreceptors as oxygenation of the blood was maintained throughout the challenge. Both the central and peripheral chemoreflex responses were generated prior to, and at 60 and 120 min after IT treatment (Fig. 1).

***Collection of blood and plasma samples and catecholamine analysis:*** At the conclusion of the electrophysiology experiments, 3-4 ml blood was withdrawn from the carotid artery and collected in heparinised tubes containing metabisulphite. Blood samples were immediately centrifuged at $4^0$C for 10 min at 900g and plasma collected and stored at -$20^0$C until analysis. Plasma adrenaline and noradrenaline were extracted onto activated alumina, eluted, and analysed with reverse phase HPLC and electrochemical detection.

## Histology

***Perfusions:*** One millilitre of heparin was injected in each rat through the venous line at the conclusion of the electrophysiology experiments, and then rats were perfused transcardially with 400 ml of ice-cold 0.9% saline followed by 400 ml of 4% paraformaldehyde solution. Brains were removed and post-fixed in the same fixative for 18-24 h.

***Sectioning and immunohistochemistry:*** Immunohistochemical analysis was done, as described previously (Bhandare et al., 2016a; Kapoor et al., 2016c), in *n* = 3 rats from both post-SE and control groups treated with IT PBS. Brainstems were sectioned coronally (40 µm thick) with a vibrating microtome (Leica, VT1200S). Sections were sequentially collected into five different pots containing a cryoprotectant solution, and stored at -$20^0$C until further processing. Histological procedures were performed on free-floating sections. Sections were rinsed, blocked, and incubated in primary antibodies for 48 h: rabbit anti-CD206 (1:2,000; Abcam, Melbourne, Victoria, Australia), goat anti-Iba1 (1:1,000; Novus Biologicals, Littleton, Colorado, USA) and mouse anti-tyrosine hydroxylase (TH) (1:100; Avanti Antibodies; (Nedoboy et al., 2016)). Sections were rinsed and CD-206 (cluster of differentiation (CD)-206 is a mannose receptor present on M2 phenotype of microglia), Iba1

(iodinised calcium binding adaptor molecule-1; a microglia/macrophage specific calcium binding protein) and TH (C1 neurons) immunoreactivity was subsequently revealed by overnight incubation with the following secondary antibodies at 1:500 dilutions (Jackson Immunoresearch Laboratories, West Grove, Pennsylvania, USA): Alexa Fluor 488-conjugated donkey anti-rabbit, Cy3-conjugated donkey anti-goat, and Cy5-conjugated donkey anti-mouse,. Sections were rinsed, mounted sequentially on glass slides, and coverslipped with Vectashield (Vector Laboratories, Burlingame, California, USA).

**Data acquisition and analysis**

***Electrophysiology data:*** Data were acquired using a Spike2 acquisition and analysis software (version 8.06; Cambridge Electronic Design), and CED 1401 ADC system (Cambridge Electronic Design). The EEG data were recorded, amplified (CWE, Incorporated, BMA-931 Bioamplifier), band-pass filtered from 1 Hz to 10 kHz, and digitised at 20 kHz with a 100x gain. The EEG raw signal was DC removed and the “gamma” frequency range (25-45 Hz) was analysed, as shown previously (Bhandare et al., 2016a). The EEG “gamma” frequency range was analysed from 5 min blocks taken 1 min before IT treatment and 60 and 120 min post-treatment. The EEG data was also manually analysed in a blinded manner for detection of seizure activity as explained above. Phrenic nerve activity was rectified and smoothed (τ 0.5 s), and analysed from 1-min blocks taken 1 min before, and 60 and 120 min after IT treatment. The phrenic nerve activity area under curve (AUC) was analysed at 60 and 120 min after IT treatment. The percent change in the AUC at 60 and 120 min were compared with the pre-treatment area that was considered as 100%. SNA was rectified and smoothed (τ 2 s), and normalized to zero by subtracting the residual activity 5-10 min after death or after nerve pinch. The integrated SNA trace was calibrated (baseline as 100% and death level as 0%) and analysed for AUC between 60 to 120 min after IT PBS, PACAP(6-38) or minocycline infusion. Mean arterial pressure (MAP) and HR were analysed from 1-min blocks taken 1 min before, and 30, 60, 90 and 120 min after IT infusion (only 120 min results are shown in graphs). Baroreflex and somatosympathetic reflex responses were analysed before, and 60, 90 and 120 min after IT treatment (Fig. 1). The percent change in baroreflex response (AUC) was calculated considering pre-treatment response as 100%. The somatosympathetic reflex response was analysed with a sigmoid curve fit analysis. A

sigmoid curve was fitted to averaged waveform of somatosympathetic response curve (both fast conducting A-fibre and slow conducting C-fibre response). The low, high, range, and slope values were calculated (only range is shown in the graph). The pre-treatment range is considered as 100% response, and percent change is calculated at 60, 90 and 120 min post-treatment. Peripheral and central chemoreflex responses were analysed as percent change in the SNA AUC at 60 and 120 min post-treatment compared to the pre-treatment response (considered as 100%).

Core body temperature, and end-tidal $CO_2$ were analysed from 1-min blocks taken 1 min before and 30, 60, 90, and 120 min after IT injection. In all animals, arterial blood gas levels ($PaCO_2$) and pH were measured 10 min before the start of the protocol, and 120 min after IT treatment. Statistical analysis was carried out in GraphPad Prism software (version 6.05). Statistical significance was determined using one-way ANOVA followed by t-tests with the Holm-Šídák correction. Multiple comparisons were done between groups. $p \leq 0.05$ was considered significant.

***Calculation of corrected QT (QTc) interval:*** ECG raw data was processed (DC remove), wherever baseline fluctuations were prominent. QT, PR, and RR intervals were analysed from the ECG recordings. Bazett formula was used for calculation of QTc interval, where the QT interval in seconds was divided by the square root of the R-R interval in seconds (Bazett, 1920). The QTc was obtained before, and 120 min after IT injection. The QTc and PR interval statistical analysis was carried out in GraphPad Prism software (version 6.05). Statistical significance was determined using one-way ANOVA between treatment groups followed by t-tests with the Holm-Šídák correction. Multiple comparisons were done between groups. $p \leq 0.05$ was considered significant.

***Histology imaging and analysis:*** Acquisition and analysis of histology images is performed as described previously (Bhandare et al., 2016a; Kapoor et al., 2016b; Kapoor et al., 2016c). In brief, all images were acquired, at 20X and 40X magnifications, using a Zeiss Axio Imager Z2 (Zeiss, Germany). A 0.16 $mm^2$ box was then placed within the imaged RVLM, and this area was used for analysis. The branch length and a number of endpoint processes of Iba1-labelled microglial cells in the vicinity of TH-labelled RVLM neurons was analysed using ImageJ plugin software. Statistical analysis was carried out using GraphPad Prism (version 6.05) for

chi-square test for goodness of fit. The proportions of CD206 labelled anti-inflammatory M2 microglia in the RVLM of post-SE rats were compared with control group. Statistical significance was determined using non-parametric Mann-Whitney test (Sokal and Rohlf, 2012).

**Results:**

**Development of spontaneous recurrent seizures in post-SE rats**

A typical spontaneous recurrent seizure with transition into ictal period is shown in Fig. 2, which is characterised by high-amplitude and showed a clear new pattern of tracing. Video-EEG-ECG recordings confirmed that 9 weeks after induction of KA-induced SE, almost all rats developed spontaneous recurrent seizures with 0.44 ± 0.07 seizures per day (range 0-3) and with duration of 19.7 ± 3.3 sec per day (Table 1). The seizure frequency and scores are highly variable across the post-SE rats as shown in Table 1. Whilst some of the post-SE animals may not have had seizures during recording period (a week), and is just could be due to the low frequency. None of the control rats (saline treatment) developed spontaneous seizures.

**Chronic seizure-induced tachycardia and HR variability changes**

The *in vivo* EEG-ECG recordings in conscious chronic epileptic rat revealed that spontaneous seizure causes a dramatic tachycardia (~500 bpm (beats per minute) compared with ~300 bpm during pre-ictal period; Fig. 3A) and was characterised by a significant variability. The HR variability was increased from 91.8% to 98.2% in post-ictal period (Fig. 3B-E). HR was significantly unstable for more than one hour after the spontaneous seizure. These changes would contribute to the development of unstable, and possibly lethal cardiovascular abnormalities.

**MAP, HR and plasma catecholamines in post-SE and control rats**

Non-invasive tail-cuff blood pressure measurements confirmed that there were no significant differences in MAP and HR interictally between post-SE (*n* = 15), and control (*n* = 9) rats (Table 2). The MAP was 125.8 ± 4.5 mmHg in post-SE rats compared to 129.3 ± 3.9 mmHg in controls (Table 2). Moreover, the systolic and diastolic blood pressure values were not significantly different between these two

groups (data not shown). The HR was 310 ± 8 bpm and 326 ± 10 bpm in post-SE and control rats, respectively (Table 2). Plasma catecholamine levels (adrenaline and noradrenaline) were also not significantly different between the groups. The plasma adrenaline was 1.6 ± 0.3 nmol/L and 1.9 ± 0.5 nmol/L in post-SE and control rats, respectively (Table 2). The noradrenaline concentration was also similar in both groups of rats; 3.4 ± 0.5 nmol/L in post-SE, and 3.9 ± 0.8 nmol/L in controls (Table 2).

**Inhibition of microglial activation, but not PACAP, attenuates higher SNA and proarrhythmogenic changes in rats with spontaneous recurrent seizures**

Our results showed that in chronically epileptic post-SE rats, the antagonism of microglial activation with minocycline at IT level significantly reduced SNA (Δ -25.0 ± 10.0%; $p \leq 0.05$) compared to PBS-treated group (Δ 10.0 ± 7.7%) (Fig. 4AI). More interestingly, IT minocycline treatment in control rats (Δ -17.1 ± 18.5%) has a similar effect to PBS-treated control rats (Δ -17.8 ± 19.8%) (Fig. 4BI). IT PACAP(6-38) does not affect SNA activity in post-SE rats (Δ -15.3 ± 10.1%) compared with PBS treatment (Fig. 4AI). Similar results were obtained in control rats where changes in SNA were non-significant in IT PACAP(6-38) (Δ -18.5 ± 8.1%), and PBS treatments (Fig. 4BI). MAP and HR remained unchanged in both post-SE, and control rats treated with IT PBS, PACAP antagonist, and microglia antagonist (Figs. 4AII-III and 4BII-III). In post-SE rats, the HR changes were similar in PBS (Δ 0 ± 9 bpm), PACAP(6-38) (Δ -8 ± 5 bpm) and minocycline (Δ 1 ± 8 bpm) treated rats (Fig. 4AIII). There was a similar pattern in control rats (Fig. 4BIII) treated with PBS (Δ 3 ± 14 bpm), PACAP(6-38) (Δ 7 ± 10 bpm) and minocycline (Δ 1 ± 7 bpm). MAP was found to be unaltered in post-SE (Fig. 4AII) and control groups of rats (Fig. 4BII) treated with PBS (Δ 0.0 ± 2.0 mmHg and Δ 6.5 ± 4.3 mmHg, respectively), PACAP(6-38) (Δ 1.3 ± 6.7 mmHg and Δ 4.7 ± 1.4 mmHg, respectively), and minocycline (Δ -4.3 ± 4.2 mmHg and Δ 13.7 ± 8.4 mmHg, respectively).

The ECG findings in post-SE rats treated with IT minocycline showed a reduction in QTc interval duration (Figs. 5AI, 5CIII). In post-SE rats, the QTc interval was significantly reduced at 120 min after minocycline treatment compared to the pre-treatment period (Δ -3.0 ± 0.5 ms; $p \leq 0.05$). The representative Poincare plot (Fig. 5CIII) clearly shows that IT minocycline treatment significantly reduced the QT interval. At 120 min post-treatment, the QTc interval in IT PBS and PACAP(6-38)

treated groups did not change compared to the pre-treatment period (Δ 1.7 ± 1.1 ms and Δ 0.5 ± 1.3 ms, respectively; Fig. 5AI) (representative Poincare plot Fig. 5CI-II). In control rats, none of the treatments (IT PBS, PACAP(6-38) or minocycline) had a significant effect on QTc interval (Fig. 5BI). The IT PBS, PACAP(6-38) and minocycline do not alter the PR interval values in post-SE and control rats (Figs. 5AII and 5BII).

We did not observe any changes in EEG activity, phrenic nerve activity, expired $CO_2$ or body temperature in any of the groups (results not shown). EEG data during electrophysiology experiments revealed that none of the post-SE or control rats had spontaneous seizures under anaesthetised experimental conditions. Blood gas analysis confirmed that $PaCO_2$ and pH were within the normal physiological range ($PaCO_2$ was 40 ± 2 and pH between 7.35-7.45) throughout the experiments.

**Neither microglia nor PACAP antagonists alter baroreflex, peripheral or central chemoreflex responses in epileptic post-SE or control rats, with varied effects on somatosympathetic responses**

A typical cardiovascular reflex response is shown in Figure 1A. The protocol involved stimulation of aortic depressor nerve (baroreflex; Fig. 1B), stimulation of sciatic nerve (somatosympathetic; Fig. 1C), peripheral chemoreflex (Fig. 1D) and central chemoreflex responses (Fig. 1E), which were repeated at 60 and/or 90 and 120 min after IT treatment. Baroreflex responses were unaffected with the antagonism of PACAP or microglia in both post-SE, and control rats at 60 min, 90 min, and 120 min post-treatment (Figs. 6AI and 6BI). 120 min after IT treatments, the %Δ AUC of baroreflex response was unchanged in post-SE rats and control rats treated with PBS (Δ 0.6 ± 1.7% and Δ 3.1 ± 0.3%, respectively), PACAP(6-38) (Δ 2.0 ± 7.9% and Δ -1.0 ± 0.5%, respectively), and minocycline (Δ 1.3 ± 2.6% and Δ 1.3 ± 1.5%, respectively).

The IT treatments in both post-SE and control rats produced varied effects on somtosympathetic reflex responses (Figs. 6AII-III and 6BII-III). Stimulation of sciatic nerve in post-SE rats treated with PBS showed significant decrease in fast (A-fibre; Fig. 6AII), and slow (C-fibre; Fig. 6AIII) conducting nerve fibre somatosympathetic responses over the time course (Δ -36.0 ± 8.3% and Δ -53.6 ± 14.3%, respectively at 120 min; $p \leq 0.05$). In post-SE rats, the A- and C-nerve fibre somatosympathetic

responses were unaffected by IT PACAP(6-38) (Δ -29.8 ± 17.5% and Δ -40.8 ± 18.4%, respectively at 120 min) and minocycline (Δ -37.4 ± 16.3% and Δ -43.8 ± 21.9%, respectively at 120 min) treatment (Figs. 6AII-III). At 60, 90 and 120 min post-treatment, the fast conducting A-fibre somatosympathetic response was decreased in control rats treated with minocycline (Δ -61.0 ± 9.9%, at 120 min; $p \leq 0.001$; Fig 6BII), whereas slow conducting C-fibre response was significantly reduced in rats treated with IT PBS (Δ -55.2 ± 9.6%, at 120 min; $p \leq 0.001$) and PACAP(6-38) (Δ -49.0 ± 3.1%, at 120 min; $p \leq 0.01$) (Fig. 6BIII).

The peripheral and central chemoreflex responses in post-SE, and control rats treated with IT PBS, PACAP(6-38), and minocycline were not altered at 60 or 120 min post treatment (Fig. 7). In post-SE rats, peripheral (Fig. 7AI) and central (Fig. 7AII) chemoreflex responses were unchanged in IT PBS (Δ 2.5 ± 10.0% and Δ 13.3 ± 3.7%, respectively), IT PACAP(6-38) (Δ 3.9 ± 3.7% and Δ -1.1 ± 3.1%, respectively), and IT minocycline (Δ 5.8 ± 2.9% and Δ 1.9 ± 3.3%, respectively) treated groups. The similar trend was noted in control rats where change in peripheral (Fig. 7BI) and central (Fig. 7BII) chemoreflex responses were Δ 3.7 ± 1.4% and Δ 3.2 ± 1.1% in IT PBS groups, respectively, Δ 5.7 ± 4.8% and Δ -10.8 ± 10.3% in IT PACAP(6-38) groups, respectively, and Δ 8.8 ± 10.0% and Δ 6.1 ± 1.8% in minocycline-treated groups, respectively.

**During spontaneous recurrent seizures, microglia are in surveillance state in the vicinity of the RVLM neurons**

The morphological analysis of microglia was carried out in post-SE and control rats (*n = 3*) in the vicinity of the RVLM neurons. The brainstem sections that contain TH-immunoreactive (ir) RVLM neurons, were labelled with CD206-ir labelled anti-inflammatory M2 phenotype of microglia, and Iba1, which is a marker for all microglia. The morphological analysis demonstrated that TH-ir neurons were surrounded with typical resting microglial cells in both groups (Fig. 8A-B). In both groups microglia appeared with a round cell body, and normal long processes with few ramifications (Fig. 8A-B). Total number of microglia in each group are shown in Table 3. Activated microglia were identified with the analysis of branch length and a number of endpoint processes. Mean branch length and a number of endpoint processes of Iba1 labelled microglia were not significantly different between vehicle

control and epileptic rats (Table 3). The proportion of anti-inflammatory M2 phenotype of microglia was 12.91 ± 3.95% in post-SE rats, which was similar in controls (8.89 ± 2.14%; Table 3). These findings revealed that microglia are in a surveillance state and there are no differences in their morphology and proportion of M2 phenotype, at least in the RVLM, between epileptic and control groups.

**Discussion:**

The study provides direct evidence that microglia play a role in mediating increased SNA, and arrhythmogenic cardiac electrophysiological changes in chronic epileptic rats. First, spontaneous seizures cause severe tachycardia with prolongation of QT interval that persisted for more than one hour after the onset of a seizure. Secondly, antagonism of microglial activation, but not PACAP, in the spinal cord significantly reduces the SNA and seizure-induced prolongation of QTc interval in epileptic rats. Control groups showed no significant changes, however large variations could be attributed to sample size. Thirdly, neither spinal PACAP nor microglia regulate baroreflex or peripheral and central chemoreflex responses in epileptic and control rats, whereas PACAP or microglia antagonist decreases either A- or C-fibre somatosymapthetic response in control rats and has no effect in post-SE rats. Fourthly, interictally epileptic rats, and controls, were normotensive with the plasma catecholamine levels in a normal range. Finally, our findings show that morphologically, microglia were in a surveillance stage in chronically epileptic rats with no difference in the number of a M2 phenotype compared with controls.

Microglia are the resident immune cells of the CNS, contributing ~10% of the total brain cell population. They respond to all types of pathological stimulus, including seizures, through activation, and adoption of either a ‘pro-inflammatory M1’ or ‘anti-inflammatory M2’ phenotype (Li et al., 2007; Lai and Todd, 2008; Loane and Byrnes, 2010; Kapoor et al., 2016a). Epileptic seizures cause extensive microglial activation in patients (Beach et al., 1995), and in animal models (Drage et al., 2002), but there is a considerable controversy surrounding the pro- (Shapiro et al., 2008) or anti-inflammatory (Mirrione et al., 2010; Eyo et al., 2014) role of microglia during and following a seizure. Previous findings demonstrated that during acute seizures, microglia protect sympathetic preganglionic neurons from excitotoxicity (Bhandare et al., 2015). Our current findings show that the SNA and prolongation of QTc interval

following spontaneous seizures were significantly reduced in epileptic rats, when the microglial activation was inhibited at the IML. These novel findings strengthen the concept that during chronic pathological insult, such as spontaneous recurrent seizures, maladaptive responses of microglia may lead to a “deleterious” activation state (M1) that triggers the release of pro-inflammatory cytokines such as IL-1β and TNFα (Benson et al., 2015), in contrast to their beneficial activation during acute insult (Fig. 9). This concept has been proposed by others (Hanisch and Kettenmann, 2007; Gao et al., 2011; Eyo et al., 2017), and is supported by previous studies (Bhandare et al., 2015; Olmos-Alonso et al., 2016). During acute seizure, microglia can acquire a “beneficial” activation state (M2) to protect an overexcited neurons, and restore the normal homeostatic condition to limit the further damage (Fig. 9), whereas pharmacological targeting of colony-stimulating factor 1 receptors during late (chronic) phase in transgenic mice inhibits microglial proliferation and prevents the progression of Alzheimer’s-like pathology (Olmos-Alonso et al., 2016).

Minocycline inhibits p38 mitogen-activated protein kinase and acts as a microglia antagonist (He et al., 2001; Tikka et al., 2001; Ueno et al., 2013). Minocycline does not produce significant effect on the neuronal activity (Wu et al., 2002; Ueno et al., 2013) or SNA (Bhandare et al., 2015) and any possible effect is nullified with inclusion of control group.

Cardiovascular autonomic dysfunction with profound arrhythmogenic effects, including prolongation of QT interval, QT dispersion, “T”-wave inversion, and tachycardia or bradycardia, are major risks for SUDEP in humans and animals with spontaneous recurrent seizures (Opherk et al., 2002; Sakamoto et al., 2008; Metcalf et al., 2009; Brotherstone et al., 2010; Powell et al., 2014b; Eastaugh et al., 2015; Lamberts et al., 2015). Activated microglia are present in post-SE rats (Shapiro et al., 2008), and during chronic periods of epilepsy in humans (Beach et al., 1995) and animals (Shapiro et al., 2008). Our electrophysiology findings suggest that during chronic epilepsy ramified or activated microglia (“M1” phenotype) might have produced pro-inflammatory cytokines, and contributed to a persistent neuroinflammation that lead to higher SNA and prolongation of QT interval (Fig. 9), which was seen even one hour after spontaneous seizure. However, microglial morphological analysis revealed no change in their phenotype at least in the vicinity of the RVLM neurons. In this paradigm, as shown recently, physiological stimulus

alert microglia (ramified) (Vinet et al., 2012), and change their spatial distribution and extent of end point processes contacting synapses without significant morphological changes (Kapoor et al., 2016c), which might be facilitating the pro-inflammatory effects during chronic epilepsy. Microglial activation into a deleterious phenotype in Parkinson's disease is responsible for chronic neuroinflammation, and progressive neurodegeneration of dopaminergic neurons (Gao et al., 2011). Thus, increased microglial activation or alertness during the post-seizure period in chronic epilepsy might mediate the expression and release of pro-inflammatory cytokines, and neuroinflammation in the IML. This might lead to severe cardiovascular autonomic dysfunction and a higher risk of malignant cardiac arrhythmias, and SUDEP, during chronic epilepsy (Fig. 9) (Kloster and Engelskjøn, 1999; Langan et al., 2000). Moreover, deleterious microglial response during chronic epilepsy might regulate the neurodegeneration, and neuronal loss in brainstem autonomic nuclei in SUDEP and TLE patients (Mueller et al., 2014). Collectively, chronic epilepsy-induced microglial activation contributes to sympathoexcitation and severe arrhythmogenic changes in rats.

PACAP is a pleiotropic neuropeptide that achieves its effect through cAMP-mediated mechanisms. PACAP produces neuroprotective effects (Shioda et al., 1998) as well as activates sympathetic efferent neurons (Farnham et al., 2008; Farnham et al., 2011; Inglott et al., 2011). Antagonism of PACAP in the IML during acute seizures cause greater sympathoexcitation in rats (Bhandare et al., 2015), suggesting its neuroprotective effect during acute seizures. Microinjection of a PACAP receptor antagonist into the RVLM during acute seizures does not alter SNA but does ameliorate the seizure-induced arrhythmogenic effects (Bhandare et al., 2016a). Our results demonstrate that antagonism of PACAP at the IML during chronic epilepsy did not alter SNA or QTc interval, which suggests that PACAP is not modulating overall sympathetic output or arrhythmogenic effects in chronic epileptic rats. This might be due to low levels of PACAP in post-SE rats under our experimental conditions. PACAP gene expression increases after seizures, and reaches maximum at 12 h (Fig. 9) (Nomura et al., 2000). During electrophysiology experiments, we did not observe spontaneous seizures, which suggest that there might not be increased PACAP levels in post-SE rats during electrophysiology recordings. However, expression of PACAP can be upregulated after-seizures during the chronic epilepsy,

which could produce either neuroprotective or excitatory effect on sympathetic preganglionic neurons as shown previously (Farnham et al., 2008; Farnham et al., 2011; Bhandare et al., 2015; Bhandare et al., 2016b; Bhandare et al., 2016a).

Cardiovascular reflexes (baroreflex, somatosympathetic-reflex and peripheral and central chemoreflex) are crucial for regulation of arterial blood pressure, blood pH, and its chemical constituents (glucose, $PaCO_2$ etc.) (Pilowsky and Goodchild, 2002; Shahid et al., 2011). The baroreflex is the first line of defence during changes in blood pressure and is impaired in epilepsy patients, and animal models (Sakamoto et al., 2005; Dütsch et al., 2006). Glutamate is a major excitatory neurotransmitter, and responsible for normal maintenance of reflex responses (Miyawaki et al., 1996; Pilowsky and Goodchild, 2002; Pilowsky et al., 2009), which also plays an important role in the development of seizure (Casillas-Espinosa et al., 2012; Powell et al., 2014a; Bhandare et al., 2016b). Heart-rate baroreflex sensitivity decreases with intracerebroventricular injection of PACAP in trout (Lancien et al., 2011), whereas in rats, PACAP agonist or antagonist microinjection into the RVLM produce no significant effect (Farnham et al., 2012). In spontaneously hypertensive rats, increased microglial activation, and pro-inflammatory cytokines in PVN causes autonomic (baroreflex) dysfunction (Masson et al., 2015). However, our findings show that neither PACAP nor microglia antagonist affect the baroreflex, peripheral or central chemoreflex response in epileptic or control rats. In control rats, the microglia antagonist decreases the fast conducting, A-fibre, somatosympathetic response, whereas the PACAP antagonist decreases the slow conducting C-fibre somatosympathetic response; none of the antagonist treatments have effects in epileptic rats. The PACAP antagonist response is consistent with our other findings where PACAP(6-38) treatment did not alter the SNA and ECG findings in chronic epileptic or control rats.

Seizure activity is accompanied with increased sympathetic output, increased plasma noradrenaline levels, tachycardia and elevated blood pressure (Read et al., 2015; Bhandare et al., 2016a). However, our non-invasive blood pressure measurements and plasma catecholamine analysis did not reveal significant differences in MAP or plasma catecholamine levels interictally between epileptic and control rats. In epileptic rats, plasma catecholamine levels are reported to peak at 48 h post-seizure and then return to normal (Read et al., 2015). Differences in species, model, seizure

type, seizure frequency, and duration might explain the non-significant differences in MAP and plasma catecholamines seen in epileptic and control rats.

Sudden cardiac death in chronic epilepsy (Kloster and Engelskjøn, 1999; Langan et al., 2000) as well as cardiorespiratory autonomic dysfunction (So et al., 2000; Opherk et al., 2002; Seyal et al., 2010) is almost always associated with seizures. Therefore, it is quite likely that activated microglia-mediated neuroinflammatory changes occurring after seizure are major contributors in central autonomic cardiorespiratory dysfunction, and potentially SUDEP (Fig. 9). Overall, the current findings suggest that spontaneous recurrent seizures in chronically epileptic rats produce tachycardia with long-term prolongation of QT interval. Microglial activation in the IML contributes to higher SNA and arrhythmogenic effects in chronic epileptic rats. These findings will help to understand the biphasic microglial response at different stages in epilepsy, and assist in tailoring treatment strategies for seizure-induced central autonomic cardiovascular dysfunction with potential implications to reduce the risk of SUDEP in patients with chronic epilepsy.

**Acknowledgements:**

Work in the Authors' laboratory is supported by grants from the Australian Research Council (Discovery Early Career Researcher Award; DE120100992), National Health and Medical Research Council of Australia (1024489, 1065485, 1082215 and 1082215). AMB and KK are supported by international Macquarie University Research Excellence Scholarships (2012219 and 2012112), The Heart Research Institute (HRI) and The University of Sydney.

**References:**

Abbott SBG, Pilowsky PM (2009) Galanin microinjection into rostral ventrolateral medulla of the rat is hypotensive and attenuates sympathetic chemoreflex. Am J Physiol-Reg I 296:1019-1026.

Ansakorpi H, Korpelainen JT, Suominen K, Tolonen U, Myllylä VV, Isojärvi JIT (2000) Interictal cardiovascular autonomic responses in patients with temporal lobe epilepsy. Epilepsia 41:42-47.

Bateman LM, Li CS, Seyal M (2008) Ictal hypoxemia in localization-related epilepsy: Analysis of incidence, severity and risk factors. Brain 131:3239-3245.

Bazett HC (1920) An analysis of the time-relations of electrocardiograms. Heart 7:353-370.

Beach TG, Woodhurst WB, MacDonald DB, Jones MW (1995) Reactive microglia in hippocampal sclerosis associated with human temporal lobe epilepsy. Neurosci Lett 191:27-30.

Benson MJ, Manzanero S, Borges K (2015) Complex alterations in microglial M1/M2 markers during the development of epilepsy in two mouse models. Epilepsia 56:895-905.

Berilgen MS, Sari T, Bulut S, Mungen B (2004) Effects of epilepsy on autonomic nervous system and respiratory function tests. Epilepsy Behav 5:513-516.

Bhandare AM, Mohammed S, Pilowsky PM, Farnham MMJ (2015) Antagonism of PACAP or microglia function worsens the cardiovascular consequences of kainic-acid-induced seizures in rats. J Neurosci 35:2191-2199.

Bhandare AM, Kapoor K, Pilowsky PM, Farnham MMJ (2016a) Seizure-induced sympathoexcitation is caused by activation of glutamatergic receptors in RVLM that also causes proarrhythmogenic changes mediated by PACAP and microglia in rats. J Neurosci 36:506-517.

Bhandare AM, Kapoor K, Farnham MMJ, Pilowsky PM (2016b) Microglia PACAP and glutamate: Friends or foes in seizure-induced autonomic dysfunction and SUDEP? Respir Physiol Neurobiol 226:39-50.

Bouilleret V, Cardamone L, Liu C, Koe AS, Fang K, Williams JP, Myers DE, O'Brien TJ, Jones NC (2011) Confounding neurodegenerative effects of manganese for in vivo MR imaging in rat models of brain insults. J Magn Reson Imaging 34:774-784.

Brifault C, Gras M, Liot D, May V, Vaudry D, Wurtz O (2015) Delayed pituitary adenylate cyclase-activating polypeptide delivery after brain stroke improves functional recovery by inducing M2 microglia/macrophage polarization. Stroke 46:520-528.

Brotherstone R, Blackhall B, McLellan A (2010) Lengthening of corrected QT during epileptic seizures. Epilepsia 51:221-232.

Casillas-Espinosa PM, Powell KL, O'Brien TJ (2012) Regulators of synaptic transmission: roles in the pathogenesis and treatment of epilepsy. Epilepsia 53 Suppl 9:41-58.

Devinsky O, Vezzani A, Najjar S, De Lanerolle NC, Rogawski MA (2013) Glia and epilepsy: Excitability and inflammation. Trends Neurosci 36:174-184.

Dlouhy BJ, Gehlbach BK, Kreple CJ, Kawasaki H, Oya H, Buzza C, Granner MA, Welsh MJ, Howard MA, Wemmie JA, Richerson GB (2015) Breathing inhibited when seizures spread to the amygdala and upon amygdala stimulation. J Neurosci 35:10281-10289.

Drage MG, Holmes GL, Seyfried TN (2002) Hippocampal neurons and glia in epileptic EL mice. J Neurocytol 31:681-692.
Dütsch M, Hilz MJ, Devinsky O (2006) Impaired baroreflex function in temporal lobe epilepsy. J Neurol 253:1300-1308.
Eastaugh AJ, Thompson T, Vohra JK, O'Brien TJ, Winship I (2015) Sudden unexpected death, epilepsy and familial cardiac pathology. J Clin Neurosci 22:1594-1600.
Eyo UB, Murugan M, Wu LJ (2017) Microglia-Neuron Communication in Epilepsy. Glia 65:5-18.
Eyo UB, Peng J, Swiatkowski P, Mukherjee A, Bispo A, Wu LJ (2014) Neuronal hyperactivity recruits microglial processes via neuronal NMDA receptors and microglial P2Y12 receptors after status epilepticus. J Neurosci 34:10528-10540.
Farnham MM, Lung MS, Tallapragada VJ, Pilowsky PM (2012) PACAP causes PAC1/VPAC2 receptor mediated hypertension and sympathoexcitation in normal and hypertensive rats. Am J Physiol-Heart C 303:910-917.
Farnham MMJ, Inglott MA, Pilowsky PM (2011) Intrathecal PACAP-38 causes increases in sympathetic nerve activity and heart rate but not blood pressure in the spontaneously hypertensive rat. Am J Physiol-Heart C 300:214-222.
Farnham MMJ, Li Q, Goodchild AK, Pilowsky PM (2008) PACAP is expressed in sympathoexcitatory bulbospinal C1 neurons of the brain stem and increases sympathetic nerve activity in vivo. Am J Physiol-Reg I 294:1304-1311.
Ficker DM, So EL, Shen WK, Annegers JF, O'Brien PC, Cascino GD, Belau PO (1998) Population-based study of the incidence of sudden unexplained death in epilepsy. Neurology 51:1270-1274.
Gao HM, Zhou H, Zhang F, Wilson BC, Kam W, Hong JS (2011) HMGB1 acts on microglia Mac1 to mediate chronic neuroinflammation that drives progressive neurodegeneration. J Neurosci 31:1081-1092.
Hanisch U-K, Kettenmann H (2007) Microglia: active sensor and versatile effector cells in the normal and pathologic brain. Nat Neurosci 10:1387-1394.
He Y, Appel S, Le W (2001) Minocycline inhibits microglial activation and protects nigral cells after 6-hydroxydopamine injection into mouse striatum. Brain Res 909:187-193.
Hellier JL, Patrylo PR, Buckmaster PS, Dudek FE (1998) Recurrent spontaneous motor seizures after repeated low-dose systemic treatment with kainate: Assessment of a rat model of temporal lobe epilepsy. Epilepsy Res 31:73-84.
Inglott MA, Farnham MMJ, Pilowsky PM (2011) Intrathecal PACAP-38 causes prolonged widespread sympathoexcitation via a spinally mediated mechanism and increases in basal metabolic rate in anesthetized rat. Am J Physiol-Heart C 300:2300-2307.
Jupp B, Williams J, Binns D, Hicks RJ, Cardamone L, Jones N, Rees S, O'Brien TJ (2012) Hypometabolism precedes limbic atrophy and spontaneous recurrent seizures in a rat model of TLE. Epilepsia 53:1233-1244.
Kapoor K, Bhandare AM, Farnham MMJ, Pilowsky PM (2016a) Alerted microglia and the sympathetic nervous system: A novel form of microglia in the development of hypertension. Respir Physiol Neurobiol 226:51-62.
Kapoor K, Bhandare AM, Mohammed S, Farnham MMJ, Pilowsky PM (2016b) Microglial number is related to the number of tyrosine hydroxylase neurons in SHR and normotensive rats. Auton Neurosci-Basic 198:10-18.

Kapoor K, Bhandare AM, Nedoboy PE, Mohammed S, Farnham MMJ, Pilowsky PM (2016c) Dynamic changes in the relationship of microglia to cardiovascular neurons in response to increases and decreases in blood pressure. Neurosci 329:12-29.

Kharatishvili I, Nissinen JP, McIntosh TK, Pitkänen A (2006) A model of posttraumatic epilepsy induced by lateral fluid-percussion brain injury in rats. Neurosci 140:685-697.

Kloster R, Engelskjøn T (1999) Sudden unexpected death in epilepsy (SUDEP): A clinical perspective and a search for risk factors. J Neurol Neurosurg Psychiatry 67:439-444.

Lai AY, Todd KG (2008) Differential regulation of trophic and proinflammatory microglial effectors is dependent on severity of neuronal injury. Glia 56:259-270.

Lamberts RJ, Blom MT, Novy J, Belluzzo M, Seldenrijk A, Penninx BW, Sander JW, Tan HL, Thijs RD (2015) Increased prevalence of ECG markers for sudden cardiac arrest in refractory epilepsy. J Neurol Neurosurg Psychiatry 86:309-313.

Lancien F, Mimassi N, Conlon JM, Mével JCL (2011) Central pituitary adenylate cyclase-activating polypeptide (PACAP) and vasoactive intestinal peptide (VIP) decrease the baroreflex sensitivity in trout. Gen Comp Endocrinol 171:245-251.

Langan Y, Nashef L, Sander JWAS (2000) Sudden unexpected death in epilepsy: A series of witnessed deaths. J Neurol Neurosurg Psychiatry 68:211-213.

Li L, Lu J, Tay SSW, Moochhala SM, He BP (2007) The function of microglia, either neuroprotection or neurotoxicity, is determined by the equilibrium among factors released from activated microglia in vitro. Brain Res 1159:8-17.

Loane DJ, Byrnes KR (2010) Role of microglia in neurotrauma. Neurotherapeutics 7:366-377.

Loane DJ, Kumar A, Stoica BA, Cabatbat R, Faden AI (2014) Progressive neurodegeneration after experimental brain trauma: Association with chronic microglial activation. J Neuropathol Exp Neurol 73:14-29.

Lotufo PA, Valiengo L, Benseñor IM, Brunoni AR (2012) A systematic review and meta-analysis of heart rate variability in epilepsy and antiepileptic drugs. Epilepsia 53:272-282.

Massey CA, Sowers LP, Dlouhy BJ, Richerson GB (2014) Mechanisms of sudden unexpected death in epilepsy: The pathway to prevention. Nat Rev Neurol 10:271-282.

Masson GS, Nair AR, Soares PPS, Michelini LC, Francis J (2015) Aerobic training normalizes autonomic dysfunction, HMGB1 content, microglia activation and inflammation in hypothalamic paraventricular nucleus of SHR. Am J Physiol-Heart C 309:1115-1122.

Metcalf CS, Poelzing S, Little JG, Bealer SL (2009) Status epilepticus induces cardiac myofilament damage and increased susceptibility to arrhythmias in rats. Am J Physiol-Heart C 297:2120-2127.

Mirrione MM, Konomos DK, Gravanis I, Dewey SL, Aguzzi A, Heppner FL, Tsirka SE (2010) Microglial ablation and lipopolysaccharide preconditioning affects pilocarpine-induced seizures in mice. Neurobiol Dis 39:85-97.

Miyawaki T, Goodchild AK, Pilowsky PM (2001) Rostral ventral medulla 5-HT1A receptors selectively inhibit the somatosympathetic reflex. Am J Physiol-Reg I 280:1261-1268.

Miyawaki T, Minson J, Arnolda L, Chalmers J, Llewellyn-Smith I, Pilowsky P (1996) Role of excitatory amino acid receptors in cardiorespiratory coupling in ventrolateral medulla. Am J Physiol-Reg I 271:1221-1230.

Morimoto K, Fahnestock M, Racine RJ (2004) Kindling and status epilepticus models of epilepsy: Rewiring the brain. Prog Neurobiol 73:1-60.

Mueller SG, Bateman LM, Laxer KD (2014) Evidence for brainstem network disruption in temporal lobe epilepsy and sudden unexplained death in epilepsy. Neuroimage Clin 5:208-216.

Müngen B, Berilgen MS, Arikanoğlu A (2010) Autonomic nervous system functions in interictal and postictal periods of nonepileptic psychogenic seizures and its comparison with epileptic seizures. Seizure 19:269-273.

Nedoboy PE, Mohammed S, Kapoor K, Bhandare AM, Farnham MMJ, Pilowsky PM (2016) pSer40 tyrosine hydroxylase immunohistochemistry identifies the anatomical location of C1 neurons in rat RVLM that are activated by hypotension. Neurosci 317:162-172.

Nei M, Ho RT, Abou-Khalil BW, Drislane FW, Liporace J, Romeo A, Sperling MR (2004) EEG and ECG in sudden unexplained death in epilepsy. Epilepsia 45:338-345.

Nilsson L, Farahmand BY, Persson PG, Thiblin I, Tomson T (1999) Risk factors for sudden unexpected death in epilepsy: a case-control study. Lancet 353:888-893.

Nomura M, Ueta Y, Hannibal J, Serino R, Yamamoto Y, Shibuya I, Matsumoto T, Yamashita H (2000) Induction of pituitary adenylate cyclase-activating polypeptide mRNA in the medial parvocellular part of the paraventricular nucleus of rats following kainic-acid-induced seizure. Neuroendocrinology 71:318-326.

Ohtaki H, Nakamachi T, Dohi K, Aizawa Y, Takaki A, Hodoyama K, Yofu S, Hashimoto H, Shintani N, Baba A, Kopf M, Iwakura Y, Matsuda K, Arimura A, Shioda S (2006) Pituitary adenylate cyclase-activating polypeptide (PACAP) decreases ischemic neuronal cell death in association with IL-6. Proc Natl Acad Sci USA 103:7488-7493.

Olmos-Alonso A, Schetters STT, Sri S, Askew K, Mancuso R, Vargas-Caballero M, Holscher C, Perry VH, Gomez-Nicola D (2016) Pharmacological targeting of CSF1R inhibits microglial proliferation and prevents the progression of Alzheimer's-like pathology. Brain 139:891-907.

Opherk C, Coromilas J, Hirsch LJ (2002) Heart rate and EKG changes in 102 seizures: Analysis of influencing factors. Epilepsy Res 52:117-127.

Papageorgiou IE, Fetani AF, Lewen A, Heinemann U, Kann O (2015) Widespread activation of microglial cells in the hippocampus of chronic epileptic rats correlates only partially with neurodegeneration. Brain Struct Func 220:2423-2439.

Pilowsky PM, Goodchild AK (2002) Baroreceptor reflex pathways and neurotransmitters: 10 Years on. J Hypertens 20:1675-1688.

Pilowsky PM, Lung MSY, Spirovski D, McMullan S (2009) Differential regulation of the central neural cardiorespiratory system by metabotropic neurotransmitters. Philos T Roy Soc B 364:2537-2552.

Ponnusamy A, Marques JLB, Reuber M (2012) Comparison of heart rate variability parameters during complex partial seizures and psychogenic nonepileptic seizures. Epilepsia 53:1314-1321.

Powell KL, Lukasiuk K, O'Brien TJ, Pitkänen A (2014a) Are alterations in transmitter receptor and ion channel expression responsible for epilepsies? Adv Exp Med Biol 813:211-229.

Powell KL, Ng C, O'Brien T, Xu SH, Williams DA, Foote S, Reid CA (2008) Decreases in HCN mRNA expression in the hippocampus after kindling and status epilepticus in adult rats. Epilepsia 49:1686-1695.

Powell KL, Jones NC, Kennard JT, Ng C, Urmaliya V, Lau S, Tran A, Zheng T, Ozturk E, Dezsi G, Megatia I, Delbridge LM, Pinault D, Reid CA, White PJ, O'Brien TJ (2014b) HCN channelopathy and cardiac electrophysiologic dysfunction in genetic and acquired rat epilepsy models. Epilepsia 55:609-620.

Qin L, Wu X, Block ML, Liu Y, Breese GR, Hong J-S, Knapp DJ, Crews FT (2007) Systemic LPS causes chronic neuroinflammation and progressive neurodegeneration. Glia 55:453-462.

Read MI, McCann DM, Millen RN, Harrison JC, Kerr DS, Sammut IA (2015) Progressive development of cardiomyopathy following altered autonomic activity in status epilepticus. Am J Physiol-Heart C 309:1554-1564.

Sakamoto K, Koizumi K, Stewart M (2005) Kainic acid seizure-evoked parasympathetic and sympathetic nerve activity and altered baroreceptor reflex responses in urethane-anesthesized rats. Int Congr 1278:419-422.

Sakamoto K, Saito T, Orman R, Koizumi K, Lazar J, Salciccioli L, Stewart M (2008) Autonomic consequences of kainic acid-induced limbic cortical seizures in rats: peripheral autonomic nerve activity, acute cardiovascular changes, and death. Epilepsia 49:982-996.

Seyal M, Bateman LM, Albertson TE, Lin TC, Li CS (2010) Respiratory changes with seizures in localization-related epilepsy: Analysis of periictal hypercapnia and airflow patterns. Epilepsia 51:1359-1364.

Shahid IZ, Rahman AA, Pilowsky PM (2011) Intrathecal orexin A increases sympathetic outflow and respiratory drive, enhances baroreflex sensitivity and blocks the somato-sympathetic reflex. Brit J Pharmacol 162:961-973.

Shapiro LA, Wang L, Ribak CE (2008) Rapid astrocyte and microglial activation following pilocarpine-induced seizures in rats. Epilepsia 49:33-41.

Shioda S, Ozawa H, Dohi K, Mizushima H, Matsumoto K, Nakajo S, Takaki A, Zhou CJ, Nakai Y, Arimura A (1998) PACAP protects hippocampal neurons against apoptosis: Involvement of JNK/SAPK signaling pathway. Ann NY Acad Sci 865:111-117.

So EL, Sam MC, Lagerlund TL (2000) Postictal central apnea as a cause of SUDEP: Evidence from near-SUDEP incident. Epilepsia 41:1494-1497.

Sokal RR, Rohlf FJ (2012) Biometry, Fourth Edition. New York: W.H. Freeman and Company.

Szalay G, Martinecz B, Lenart N, Kornyei Z, Orsolits B, Judak L, Csaszar E, Fekete R, West BL, Katona G, Rozsa B, Denes A (2016) Microglia protect against brain injury and their selective elimination dysregulates neuronal network activity after stroke. Nat Commun 7:11499.

Tikka T, Fiebich BL, Goldsteins G, Keinänen R, Koistinaho J (2001) Minocycline, a tetracycline derivative, is neuroprotective against excitotoxicity by inhibiting activation and proliferation of microglia. J Neurosci 21:2580-2588.

Ueno M, Fujita Y, Tanaka T, Nakamura Y, Kikuta J, Ishii M, Yamashita T (2013) Layer v cortical neurons require microglial support for survival during postnatal development. Nat Neurosci 16:543-551.

Vinet J, van Weering HRJ, Heinrich A, Kälin RE, Wegner A, Brouwer N, Heppner FL, van Rooijen N, Boddeke HWGM, Biber K (2012) Neuroprotective function for ramified microglia in hippocampal excitotoxicity. J Neuroinflamm 9:27.

Vivash L, Gregoire MC, Bouilleret V, Berard A, Wimberley C, Binns D, Roselt P, Katsifis A, Myers DE, Hicks RJ, O'Brien TJ, Dedeurwaerdere S (2014) In vivo measurement of hippocampal GABAa/cBZR density with [18F]-flumazenil PET for the study of disease progression in an animal model of temporal lobe epilepsy. PLoS One 9:e86722.

Wada Y, Nakamachi T, Endo K, Seki T, Ohtaki H, Tsuchikawa D, Hori M, Tsuchida M, Yoshikawa A, Matkovits A, Kagami N, Imai N, Fujisaka S, Usui I, Tobe K, Koide R, Takahashi H, Shioda S (2013) PACAP attenuates NMDA-induced retinal damage in association with modulation of the microglia/macrophage status into an acquired deactivation subtype. J Mol Neurosci 51:493-502.

WHO (2005) Atlas: Epilepsy care in the world. In: (Department of Mental Health and Substance Abuse WHO, ed). Geneva.

Wu DC, Jackson-Lewis V, Vila M, Tieu K, Teismann P, Vadseth C, Choi DK, Ischiropoulos H, Przedborski S (2002) Blockade of microglial activation is neuroprotective in the 1-methyl-4-phenyl-1,2,3,6-tetrahydropyridine mouse model of Parkinson disease. J Neurosci 22:1763-1771.

**Legends:**

**Figure 1:** *In vivo* effects of IT minocycline treatment in post-SE rat on cardiovascular reflex responses. A typical response of stimulation of aortic depressor nerve (ADN) (B), sciatic nerve (SN) (C), peripheral chemoreceptors (D) and central chemoreceptors (E) on the SNA and on HR, end-tidal $CO_2$, blood pressure, EEG and SNA activity (A). The protocol was repeated at 60, and/or 90 and 120 min after IT treatment.

**Figure 2:** A typical spontaneous recurrent seizure (top) with a transition into ictal period (bottom) in epileptic rat.

**Figure 3:** The spontaneous seizure-induced tachycardia and heart rate variability. The effect of spontaneous seizure on HR (A) during *in vivo* EEG-ECG recordings in post-SE rat. The spontaneous seizure produced significant tachycardia along with increased variability in HR (B-E) during post-ictal period.

**Figure 4:** *In vivo* effects of IT PBS, PACAP(6-38) and minocycline treatment in post-SE and control rats. Change in SNA (AUC) between 60 and 120 min post treatment in post-SE (AI) and control (BI) rats. The changes in MAP (mmHg) at 120 min post IT treatment in post-SE (AII) and control (BII) rats, and HR (bpm) at 120 min after IT treatment in post-SE (AIII) and control (BIII) rats. Statistical significance was determined using one-way ANOVA followed by t-tests with a Holm Šídák correction. Data expressed as mean ± SEM. *$p \leq 0.05$ compared with IT PBS treated post-SE group.

**Figure 5:** *In vivo* effects of IT PBS, PACAP(6-38) and minocycline treatment on ECG activity. Group data showing effect of IT PBS, PACAP(6-38) and minocycline treatment on: changes in corrected QT interval (Δ QTc) (ms) (AI) and PR interval (Δ PR) (ms) (AII) at 120 min post treatment compared to the pre-treatment period in post-SE rats; and changes in QTc interval (Δ QTc) (ms) (BI) and PR interval (Δ PR) (ms) (BII) at 120 min post treatment compared to the pre-treatment period in control rats. Representative Poincare plots illustrate changes in QT interval in post-SE rats from three different groups treated with IT PBS (CI), PACAP(6-38) (CII) and minocycline (CIII). IT PBS (CI) and PACAP(6-38) (CII) treatment in post-SE rats does not alter the QT interval, whereas antagonism of microglial activity significantly

reduces the QT interval (CIII) in post-SE rats. Statistical significance was determined using one-way ANOVA followed by t-tests with a Holm Šídák correction. Data expressed as mean ± SEM. *$p \leq 0.05$ compared with IT PBS treated post-SE group.

**Figure 6:** *In vivo* effects of IT PBS, PACAP(6-38) and minocycline treatment on baroreflex and somatosympathetic reflex responses in post-SE and control rats. The % change in baroreflex response at 60, 90 and 120 min post IT treatment compared to pre-treatment period in post-SE (AI) and control rats (BI). Effect of IT treatment on % change in fast conducting (A-fibre) somatosympathetic response at 60, 90 and 120 min post treatment compared to pre-treatment period in post-SE (AII) and control (BII) rats. The % change in slow conducting (C-fibre) somatosympathetic response at 60, 90 and 120 min post IT treatment compared to pre-treatment period in post-SE (AIII) and control (BIII) rats. Statistical significance was determined using one-way ANOVA followed by t-tests with a Holm Šídák correction. Data expressed as mean ± SEM. *$p \leq 0.05$ compared with the pre-treatment time-point in post-SE group. $^{###}p \leq 0.001$, $^{##}p \leq 0.01$, $^{#}p \leq 0.05$ compared with the pre-treatment time-point in control group.

**Figure 7:** *In vivo* effects of IT PBS, PACAP(6-38) and minocycline treatment on peripheral and central chemoreflex responses in post-SE and control rats. The % change in peripheral (AI) and central (AII) chemoreflex response at 60 and 120 min post IT treatment compared to pre-treatment period in post-SE rats. The % change in peripheral (BI) and central (BI) chemoreflex response at 60 and 120 min post IT treatment compared to pre-treatment period in control rats. Statistical significance was determined using one-way ANOVA followed by t-tests with a Holm Šídák correction. Data expressed as mean ± SEM.

**Figure 8:** Fluorescence images of the RVLM area containing $TH^+$-ir (red), Iba-1 labelled microglia (yellow) and CD206-labelled M2 microglial cells (green) in post-SE (A) and control (B) rats. Scale bar, 20 µm. In both groups $TH^+$-ir neurons (red) were surrounded with microglia with its round cell body and normal appearing processes with few ramifications (closed arrow) and no change in number of anti-inflammatory M2 microglia (open arrow).

**Figure 9:** A proposed mechanism of action of microglia and PACAP on sympathetic neurons at the IML during acute and chronic seizures, and its possible outcomes.

Time scale on x-axis is variable from hours to days. Under normal conditions, highly motile “surveilling” microglia continuously survey their microenvironment through direct contact with neuronal synapses and exchange molecular signals. Microglia can immediately sense the disturbed functional and structural integrity of neurons during conditions, such as seizures. Upon detection of these trigger that are higher than the activation threshold, microglia respond through reorganisation of their processes and activity profile. During acute seizures, microglia might acquire “beneficial” activation state (M2) and produce neurotropic factors, such as IL-10 and TGF-β, to protect the overexcited neurons, and limit further damage and restore normal homeostatic condition. Seizure also triggers synthesis and release of PACAP, which peaks at 12 h post seizure, and produce either neuroprotective or excitatory effects on sympathetic neurons at IML. However, chronic seizures may trigger more drastic changes in functional phenotype of microglia. During chronic seizures, maladaptive responses of microglia may lead to “deleterious” activation state (M1) that triggers release of inflammatory molecules such as IL-1β and TNFα. This could be the mechanism for increased risk of SUDEP during chronic phase of epilepsy, and specifically during post-seizure period (as shown in orange) that is associated with central autonomic cardiovascular dysfunctions such as increased SNA and proarrhythmogenic changes.

**Table 1:** Spontaneous seizure frequency and duration in post-SE chronic epileptic rats. Seizure frequency and duration per day in IT PBS, PACAP(6-38) and minocycline treated post-SE rats. In each group *n* = 5. Data expressed as mean ± SEM.

**Table 2:** The cardiovascular activity and catecholamine levels in post-SE chronic epileptic rats compared to control. MAP (mmHg) and HR (bpm) in post-SE, and control rats recorded under conscious conditions. Plasma adrenaline (nmol/L) and noradrenaline (nmol/L) concentration in post-SE and control group of rats. Statistical significance was determined using unpaired t-test. Data expressed as mean ± SEM.

**Table 3:** Morphological analysis of fluorescence images of the RVLM area containing $TH^+$-ir, Iba-1 labelled microglia and CD206-labelled M2 microglial cells in post-SE and control rats. In both groups, there are no changes in number of Iba-1 labelled

microglia, number of anti-inflammatory M2 microglia or their morphology. Data expressed as mean ± SEM.

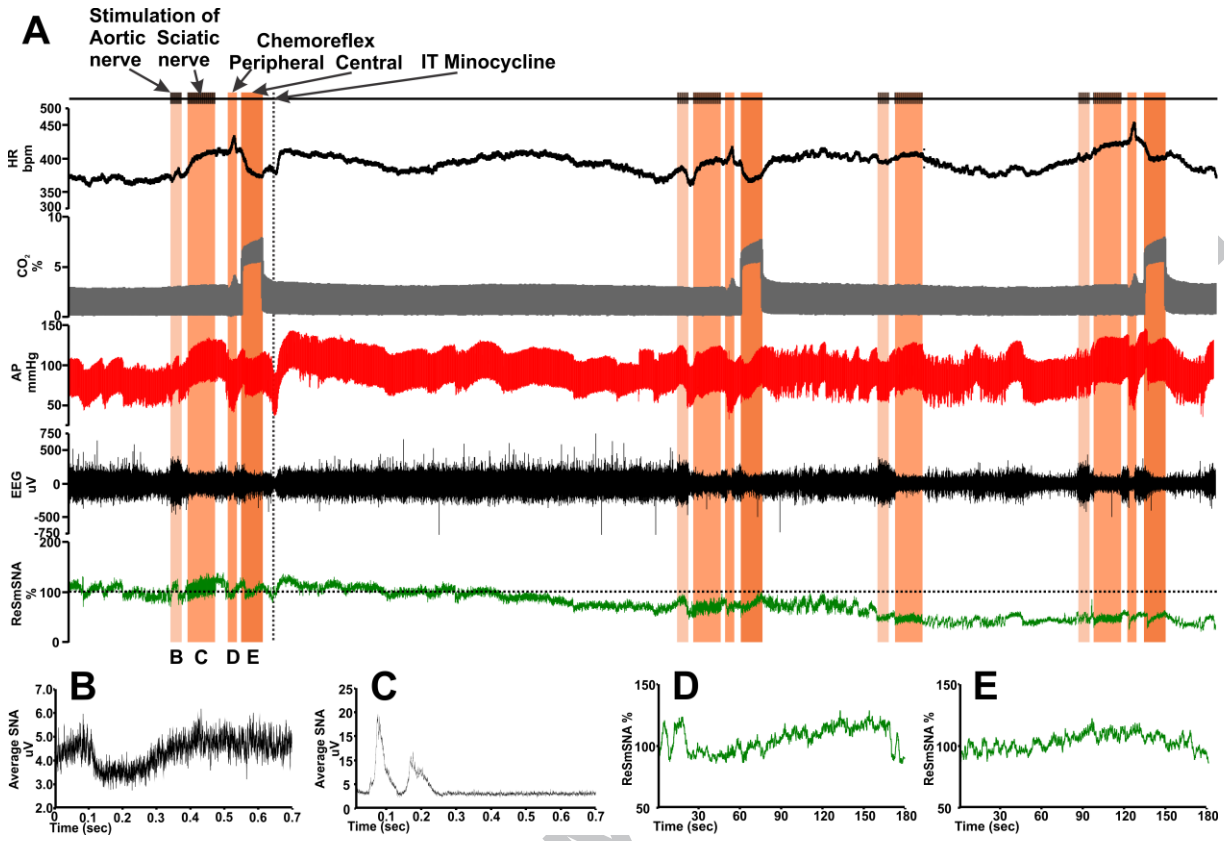

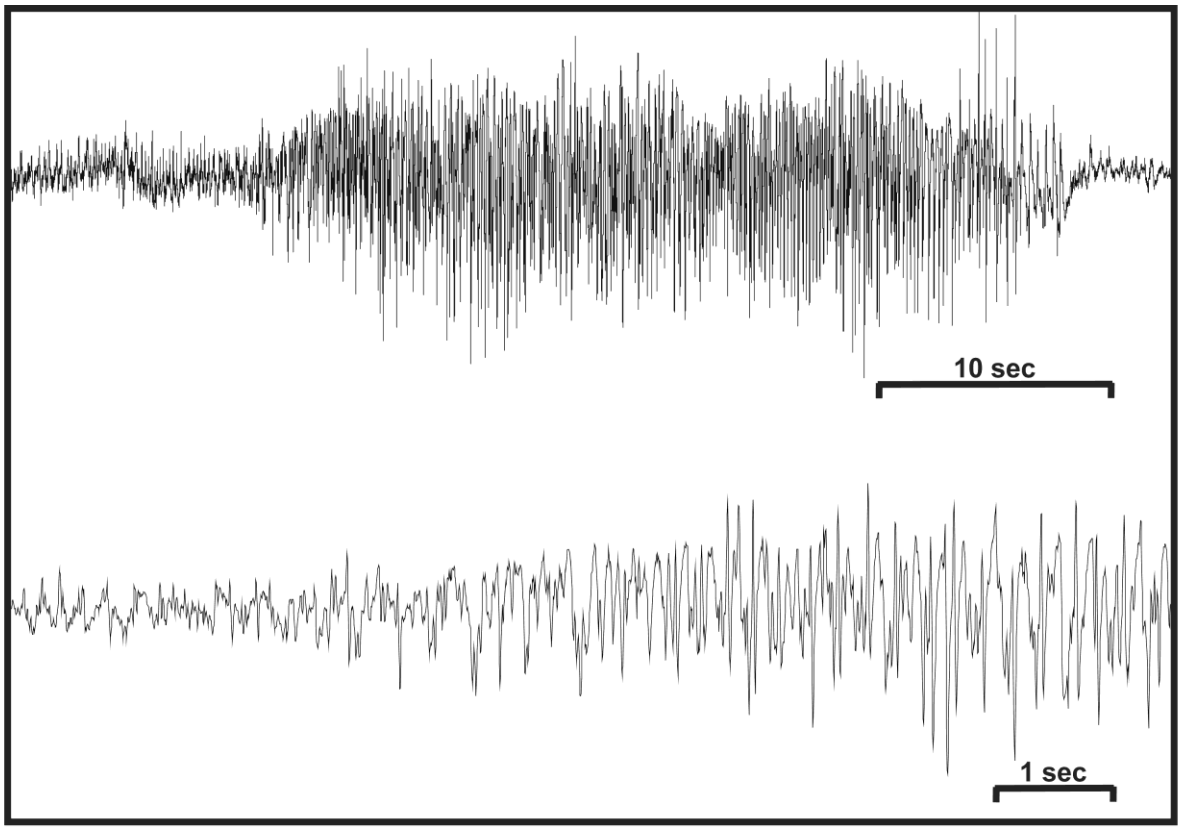


**A typical spontaneous seizure in Post-SE rat**

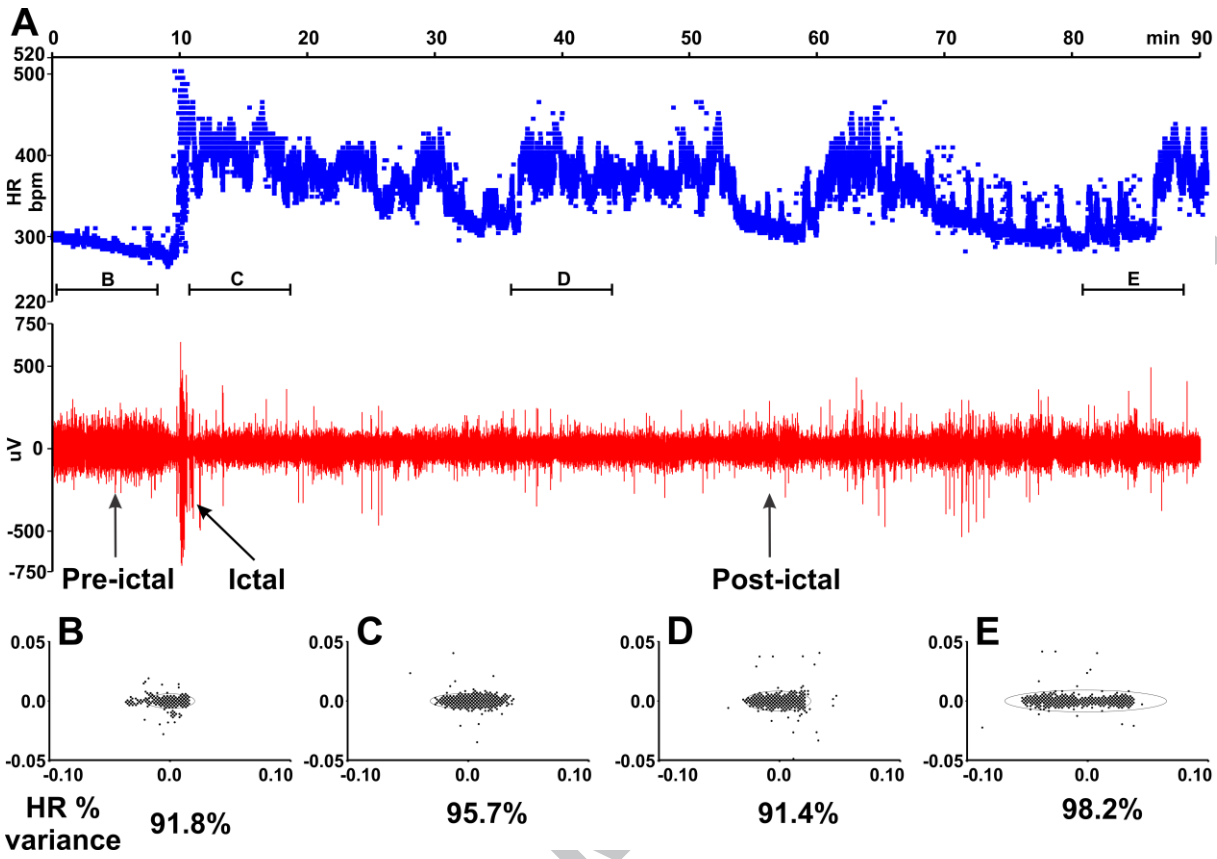

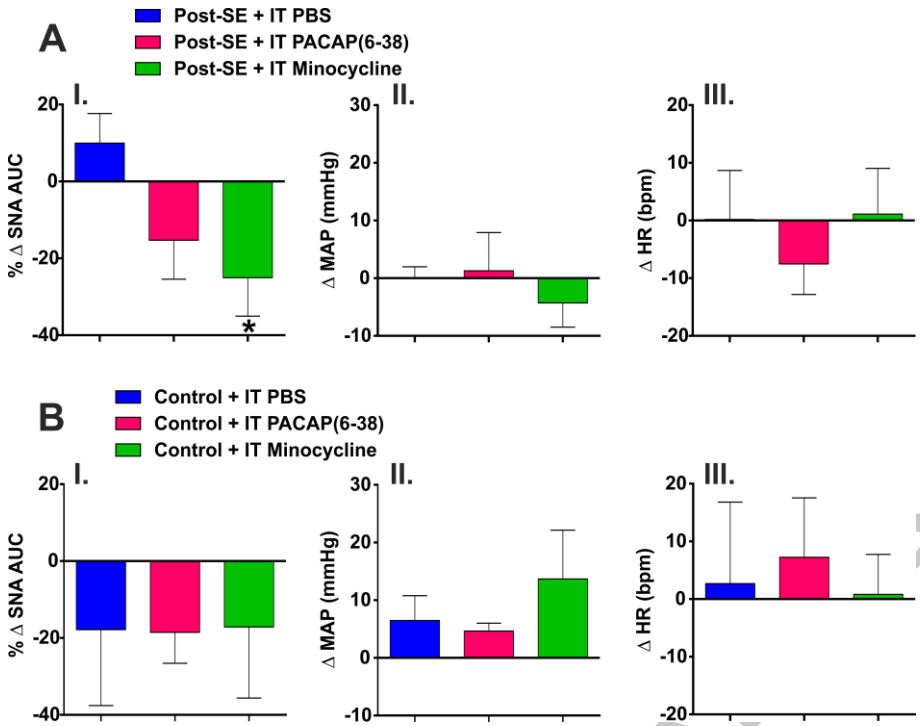

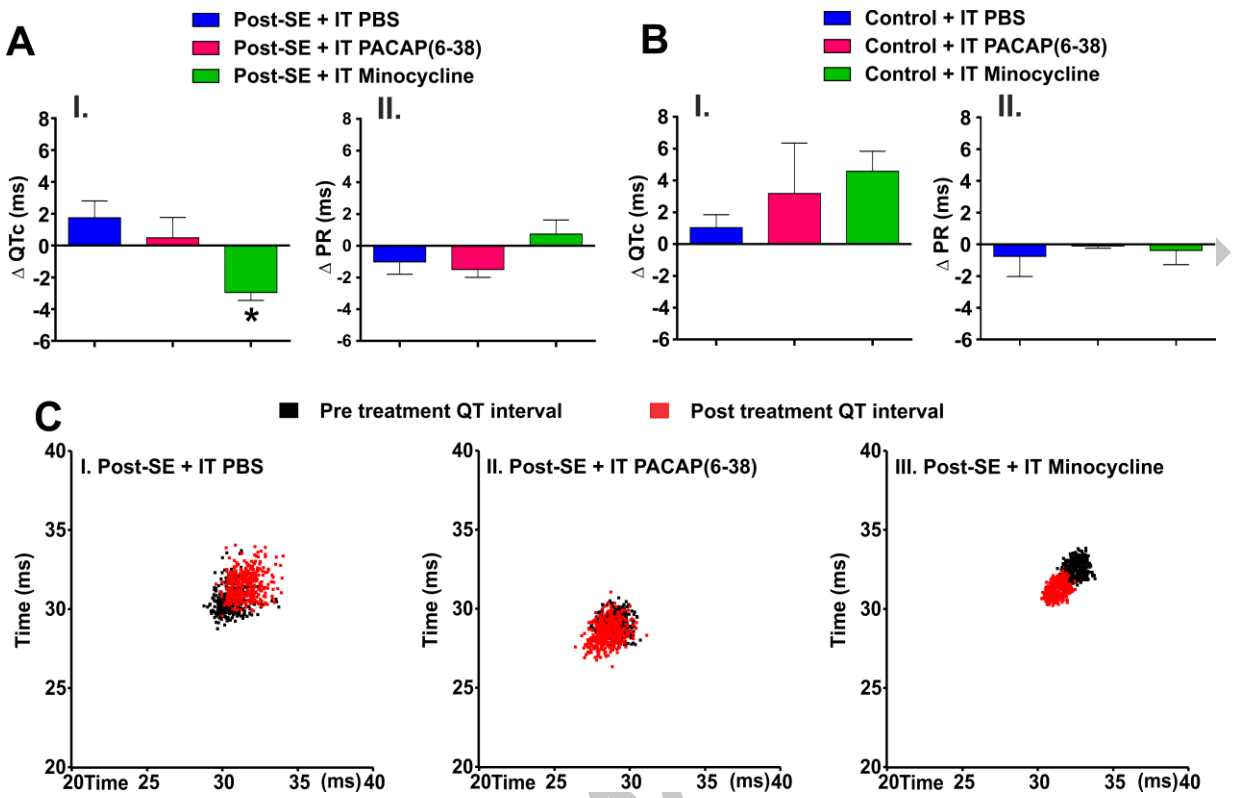

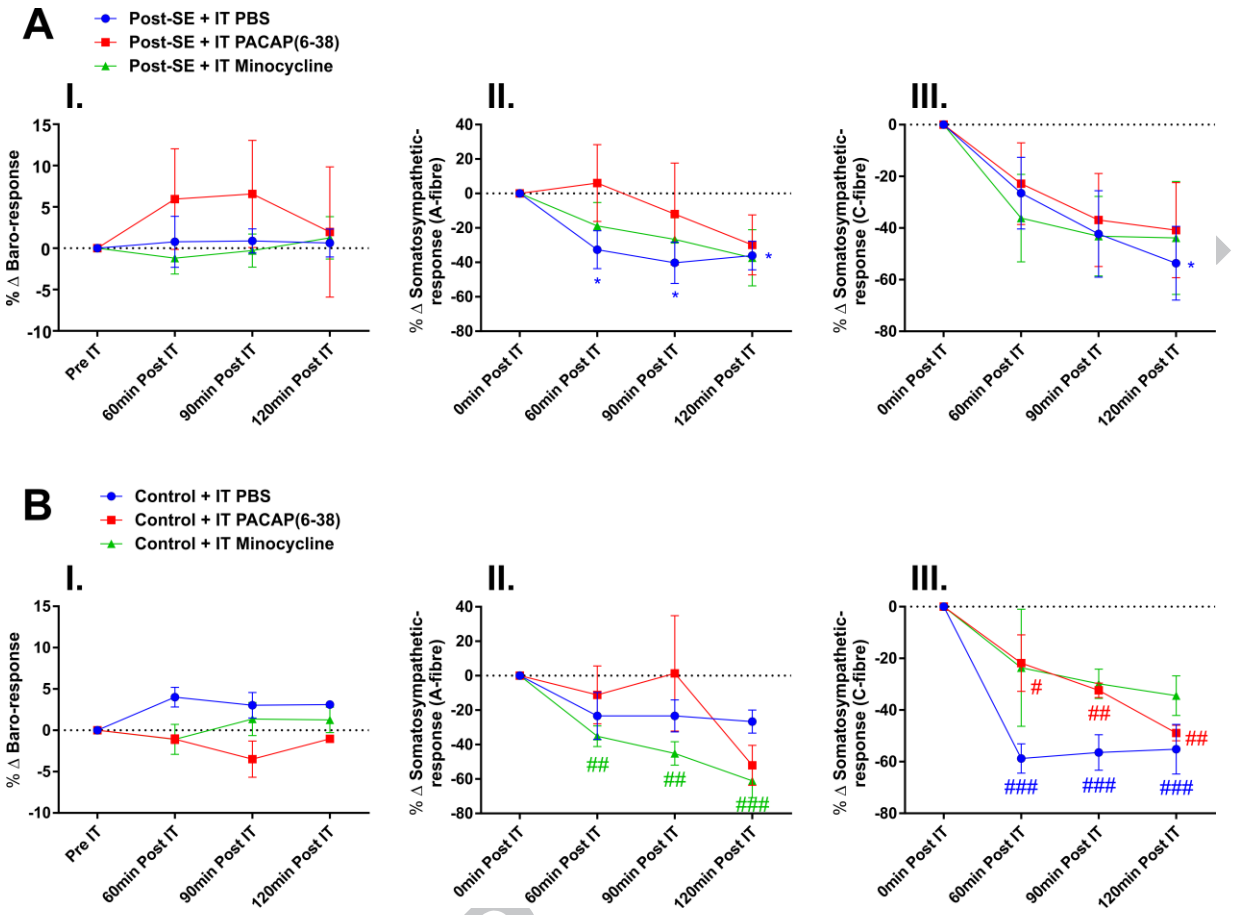

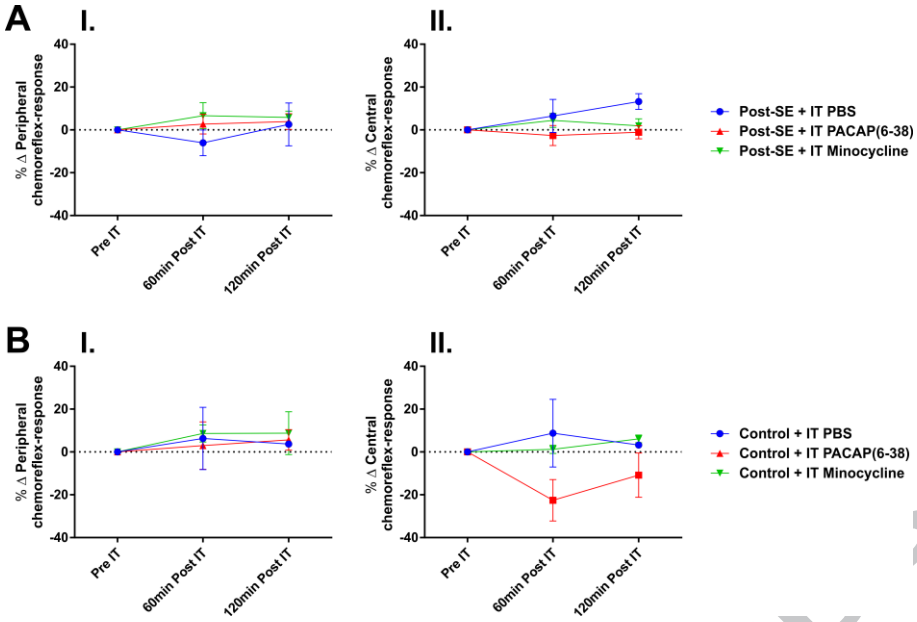

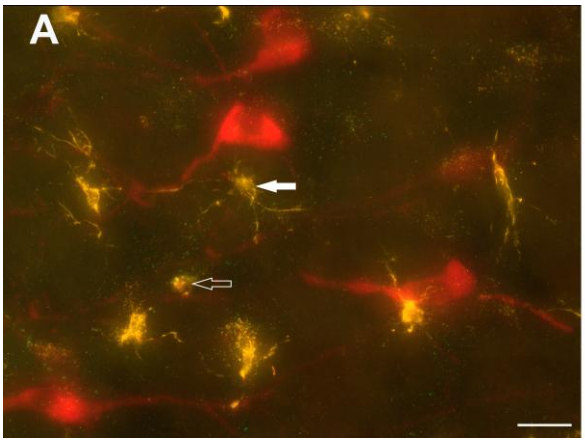


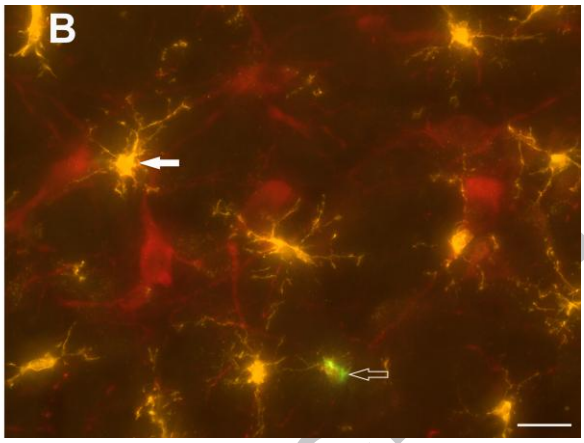

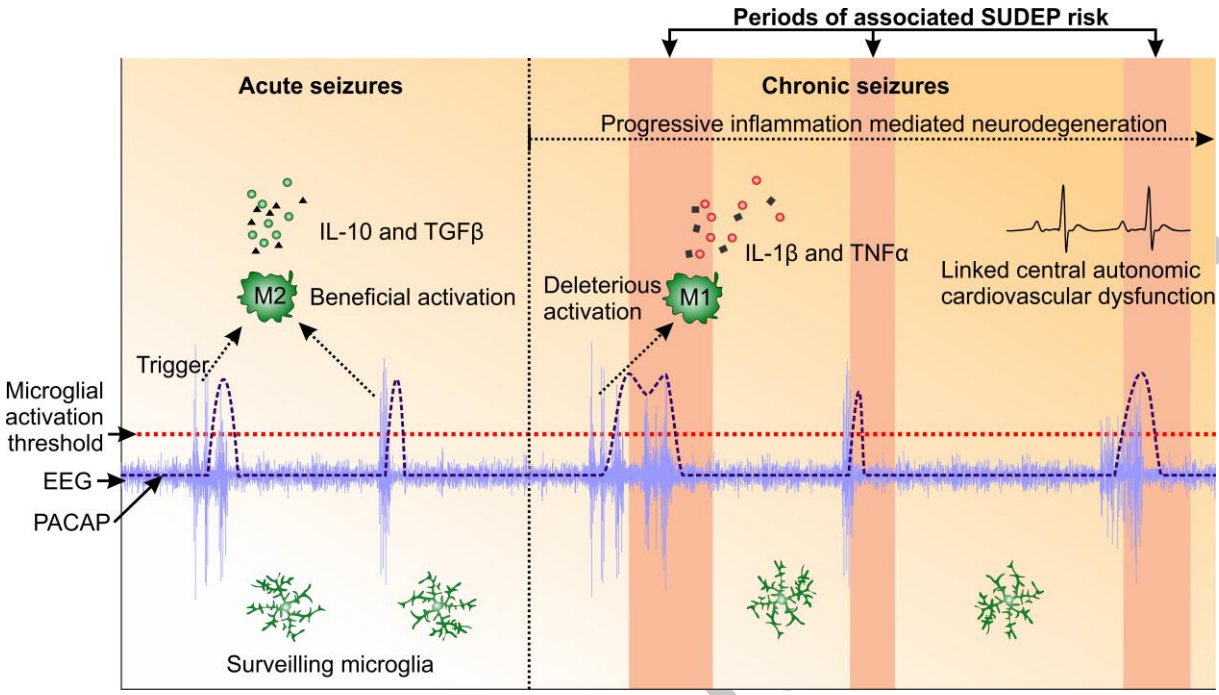

Table 1:

| Post SE + IT PBS | | | | | |
|---|---|---|---|---|---|
| Animal No. | 1 | 2 | 3 | 4 | 5 |
| No. of seizures/day | 0.29 ± 0.18 | 0.50 ± 0.50 | # | 0.43 ± 0.20 | # |
| Seizure duration (sec)/ day | 13.57 ± 8.87 | 20.50 ± 20.50 | # | 21.71 ± 10.36 | # |
| Post SE + IT PACAP (6-38) | | | | | |
| Animal No. | 1 | 2 | 3 | 4 | 5 |
| No. of seizures/day | 1.00 ± 0.53 | 0.71 ± 0.29 | 0.50 ± 0.50 | 0.57 ± 0.30 | 0.17 ± 0.17 |
| Seizure duration (sec)/ day | 44.71 ± 24.34 | 30.29 ± 12.74 | 25.0 ± 25.0 | 33.57 ± 16.89 | 5.0 ± 5.0 |
| Post SE + IT Minocycline | | | | | |
| Animal No. | 1 | 2 | 3 | 4 | 5 |
| No. of seizures/day | 0.86 ± 0.26 | 0.71 ± 0.18 | 0.14 ± 0.14 | # | 0.43 ± 0.20 |
| Seizure duration (sec)/ day | 31.14 ± 9.27 | 26.14 ± 7.16 | 4.57 ± 4.57 | # | 24.43 ± 12.39 |

# Seizures were not detected in the rat during the recording period.

Table 2:

| Treatment group | Post-SE | Control |
|---|---|---|
| MAP (mmHg) | 125.80 ± 4.49 | 129.3 ± 3.9 |
| HR (bpm) | 310 ± 8 | 326 ± 10 |
| Adrenaline (nmol/L) | 1.58 ± 0.31 | 1.9 ± 0.49 |
| Noradrenaline (nmol/L) | 3.38 ± 0.51 | 3.93 ± 0.78 |

Table 3:

| Treatment group | Post-SE | Control |
|---|---|---|
| No. of microglia | 241 | 233 |
| No. of end processes/microglia | 403 ± 76 | 478 ± 122 |
| Branch length (µm)/microglia | 197.60 ± 5.69 | 224.90 ± 12.24 |
| % CD206 labelled microglia | 12.91 ± 3.95 | 8.89 ± 2.14 |

**Highlights:**

- Epilepsy-induced altered cardiovascular function, regulated by autonomic nervous system, is a major cause of death.
- Chronic spontaneous seizures in rats produce profound proarrhythmogenic effects.
- In epileptic rats, proarrhythmogenic and sympathoexcitatory effects are mediated by action of microglia at spinal cord.
- Neither PACAP nor microglia regulate the major cardiovascular reflex responses in epileptic rats.
- Modifying the microglial activity in epileptics might produce sympathoprotective and eventually cardioprotective effects.